

# Osthole enhances the bone mass of senile osteoporosis and stimulates the expression of osteoprotegerin by activating $\beta$ -catenin signaling

**Zhen-Xiong Jin**

Longhua hospital

**Xin-Yuan Liao**

spine center

**Wei-Wei Da**

longhua hospital

**Yong-Jian Zhao**

shanghai university of traditional chinese medicine

**Xiao-Feng Li**

Shanghai University of Traditional Chinese Medicine

**Dezhi Tang** (✉ [dzt702@163.com](mailto:dzt702@163.com))

longhua hospital

---

## Research

**Keywords:** Osthole,  $\beta$ -catenin, Osteoprotegerin, Osteoclast, Osteoporosis

**Posted Date:** January 26th, 2021

**DOI:** <https://doi.org/10.21203/rs.3.rs-133397/v2>

**License:**   This work is licensed under a Creative Commons Attribution 4.0 International License.

[Read Full License](#)

---

**Version of Record:** A version of this preprint was published on February 27th, 2021. See the published version at <https://doi.org/10.1186/s13287-021-02228-6>.

# Abstract

**Introduction** Osthole has a potential therapeutic application for anti-osteoporosis. The present study verified whether osthole downregulates osteoclastogenesis via targeting OPG.

**Methods** In vivo, 12-month-old male mice were utilized to evaluate the effect of osthole on bone mass. In vitro, bone marrow stem cells (BMSCs) were isolated and extracted from 3-month-old OPG<sup>-/-</sup> mice and the littermates of OPG<sup>+/+</sup> mice. calvaria osteoblasts were extracted from 3-day-old C57BL/6J mice or 3-day-old OPG<sup>-/-</sup> mice and the littermates of OPG<sup>+/+</sup> mice.

**Results** Osthole significantly increased the gene and protein levels of OPG in primary BMSCs in a dose-dependent manner. The deletion of the *OPG* gene did not affect  $\beta$ -catenin expression. The deletion of the  $\beta$ -catenin gene inhibited OPG expression in BMSCs, indicating that osthole stimulates the expression of OPG via activation of  $\beta$ -catenin signaling.

**Conclusion** Osthole attenuates osteoclast formation by stimulating the activation of  $\beta$ -catenin-OPG signaling and could be a potential drug for the senile osteoporosis.

## Introduction

Osteoporosis is a systematic skeletal disease that thins and weakens the bones to the point that they become fragile and break easily. It is one of the most disabling consequences of aging [1,2]. Hip fractures and vertebral fractures are strongly associated with reduction in bone mineral density (BMD) and have been considered the prototypical osteoporotic fractures [3]. In 2010, about 2.7 million hip fractures occurred worldwide, and about half of these (51%) were considered preventable [4,5]. However, the incidence of all other fractures (non-hip, non-vertebral) is marked, and collectively these fractures result in large economic costs for the population [6]. Fractures show symptoms of pain and an inability to bear weight and almost always require surgical fixation [7]. In addition, the patient's functional status and quality of life are reduced, with a high risk for short-term mortality, as well as large medical expenses [8,9].

Estrogen replacement therapy is effective in increasing osteoblast activity but also increases the incidence of breast and uterine cancer [10,11]. Phytoestrogens have attracted attention due to the potential impacts on the prevention and treatment of osteoporosis. Osthole, a coumarin derivative extracted from *Cnidium monnieri* and *Angelica* of Chinese herbal medicine, has an estrogenic effect in preventing bone loss in ovariectomized rats [12,13]. Several studies have confirmed a wide range of pharmacological activities of osthole in humans, such as anti-cancer activity, antihypertensive, anti-arrhythmic, anti-inflammatory, and anti-infection properties; it also promotes osteoblast differentiation [14-16].

Bone marrow stem cells (BMSCs) differentiate into osteogenic, fat, cartilage, and nerve-like cells, with robust in vitro expansion capacity, as well as the potential for multi-directional differentiation [17,18]. The underlying mechanisms have been studied using recent technological advances in cell labeling and

tracing [19,20]. Subsequently, the lineage tracing methods proposed that bone marrow cells expressing myxovirus resistance-1 (Mx1) harbor the characteristics of BMSCs. The Mx1 protein can restrict several viruses independent of the expression of other interferon (IFN)-induced genes. These cells respond to tissue stress and migrate to the sites of injury, supplying new osteoblasts during fracture healing [21]. Leptin receptor (LepR) is also another marker for identifying BMSCs. LepR-positive cells have been shown to produce osteoblasts and adipocytes in bone marrow [22]. In addition, cells expressing gremlin-1 have been isolated from bone marrow; these cells are capable of bone formation rather than adipogenesis [23]. Thus BMSCs are widely used in clinical research at the cellular level of bone and cartilage tissues, including cartilage repair.

Our previous study demonstrated that osthole significantly stimulated osteoblast differentiation and bone formation by the activation of Wnt/ $\beta$ -catenin-Bmp2 signaling [24]. The previous meta-analysis showed that BMSCs promote bone cell maturation, ossification, and restore bone mechanical properties in osteoporotic fractures [25]. Although osthole can promote bone formation, its effect on bone resorption and the underlying mechanism is yet to be elucidated. In this study, we performed the in vivo and in vitro experiments to examine the effect of osthole on osteoclast formation.

## Materials And Methods

### Mice and reagents

All animal protocols were approved by the Institutional Review Board of Longhua Hospital, Shanghai University of Traditional Chinese Medicine (China). C57BL/6J wild-type mice, Osteoprotegerin (OPG) knockout (KO) mice, and OPG wild-type (WT) mice were purchased from the Shanghai Bio model Organism Science and Technology Development Co., Ltd (China). Osthole, with 98% purity, was purchased from the Shanghai Institute for Drug and Quarantine Bureau. The reagents used in the experiment are listed in Table S1.

### Animal study

Six-month-old C57BL/6 mice, specific pathogen-free (SPF), were purchased from the Institute of Zoology, Chinese Academy of Sciences. Four months later, C57BL/6 mice of 1-month-old were purchased again, and the experiment was performed when the mice were 3- and 12-months-old. Next, the 12-month-old male mice were randomized equally (n=6) into two groups: treatment and control group. The treatment group was intervened with osthole (5 mg/kg/day) by intraperitoneal injection once a day for 4 weeks, and the control group was intervened with vehicle (corn oil) by intraperitoneal injection once a day for 4 weeks. After sacrifice, the lumbar vertebrae were harvested for evaluation.

### Microcomputed tomography ( $\mu$ CT) analysis

The fourth lumbar vertebra (L4) was scanned at 18- $\mu$ m voxel size using the  $\mu$ CT scanner ( $\mu$ CT80, Scanco Medical AG, Bassersdorf, Switzerland). The trabecular bone under the growth plate was segmented using

a contouring tool, and the contours were morphed automatically to segment the trabecular bone on all the 100 slices. The three-dimensional (3D) images were reconstructed and analyzed using the software of the  $\mu$ CT system.

### **Histological and histomorphometric assays**

The fifth lumbar vertebra (L5) was fixed in 4% paraformaldehyde, decalcified, dehydrated, cleared with dimethyl benzene, and embedded in paraffin. At least three consecutive 7-mm sections were obtained from the coronal planes and subjected to tartrate resistant acid phosphatase (TRAP) staining to identify osteoclasts. The histomorphometric assay was performed to determine the number of osteoclasts and the proportion of osteoclast surface using an image auto-analysis system (Olympus BX50; Japan).

### **Immunohistochemical staining**

The paraffin sections of L3 were deparaffinized by immersing the tissue in xylene, fixing with 4% paraformaldehyde for 15 min, and permeabilizing with 0.5% Triton X-100 for 15 min, followed by fixation with 4% paraformaldehyde for an additional 5 min. Then, the sections were incubated with rabbit anti-OPG monoclonal antibody (1:50) and rabbit anti- $\beta$ -catenin monoclonal antibody (1:50) at 4 °C overnight and then with horseradish peroxidase (HRP)-conjugated secondary antibody for 30 min. Finally, the slides were mounted and examined using an Image Analysis System (Olympus BX50).

### **Cell culture and treatment**

Primary BMSCs, extracted from 3-month-old OPG<sup>-/-</sup> mice and the littermates of OPG<sup>+/+</sup> mice, were cultured by incubation with macrophage colony-stimulating factor (M-CSF) and receptor activator of nuclear factor (NF)- $\kappa$ B-ligand (RANKL) for 1 week, and then treated with various doses (0.5–100  $\mu$ M) of osthole for 48 h. Transgenic mice were presented by Professor Chen, Department of Orthopedics, University of Rochester. Primary calvaria osteoblasts, extracted from 3-day-old C57BL/6J mice or 3-day-old OPG<sup>-/-</sup> mice and the littermates of OPG<sup>+/+</sup> mice

### **TRAP staining**

Primary BMSCs were seeded in a 96-well plate at a density of  $3 \times 10^5$ /mL and treated with M-CSF (44 ng/mL) and RANKL (100 ng/mL) in the presence or absence of osthole (100  $\mu$ M). The medium was changed every 3 days. After 7-day incubation, the cells were fixed and subjected to TRAP staining to calculate the number of multinuclear ( $\geq 3$  nuclei) osteoclasts.

### **Real time-quantitative polymerase chain reaction (qPCR) analysis**

Primary calvaria osteoblasts, extracted from 3-day-old C57BL/6J mice, were seeded in 6-well plates at a density of  $1 \times 10^6$  cells/well. After 2-day culture, the cells were treated with various doses of osthole (1–100  $\mu$ M) or vehicle for 48 h. Total cellular mRNA was isolated using the RNeasy Mini Kit (Qiagen Corporation, Valencia, CA). An equivalent of 1 mg of total RNA was reverse-transcribed into cDNA using

the iScript cDNA synthesis kit (Bio-Rad Laboratories, Inc, Hercules, CA). qPCR analysis was carried out using Absolute QPCR SYBR Green Master Mix in a total volume of 20  $\mu$ L reaction containing 1  $\mu$ L of the diluted (1:5) reverse transcription product in the presence of sense and antisense primers of target genes listed as Table 1.  *$\beta$ -actin* served as the internal reference gene. The reaction was as follows: polymerase activation at 95 °C for 15 min, followed by 45 cycles of 95 °C for 20 s, 58 °C for 20 s, and 72 °C for 30 s. All reactions were performed in triplicate.

### **Western blotting analysis**

Primary calvaria osteoblasts, isolated from 3-day-old OPG<sup>-/-</sup> homozygous mice and the littermates of OPG<sup>+/+</sup> mice, were seeded in 6-well plates at a density of  $1 \times 10^6$  cells/well. Cells were treated with osthole (100  $\mu$ M) or vehicle for 48 h and cell lysates were extracted using protein extraction reagents (PER) (Thermo Scientific, Waltham, MA, USA). The protein concentration is 10  $\mu$ g, and by Sodium Dodecyl Sulfonate-Polyacrylamide gel electrophoresis (SDS-PAGE) and the 10% of gel. Proteins were transferred onto a PVDF membrane (Bio-Rad, Hercules, CA, USA). Subsequently, the membrane was blocked with 5% non-fat milk in Phosphate Buffered Saline and Tween-20 (PBST) for 1 h at room temperature and probed with primary antibodies overnight at 4 °C, followed by HRP-conjugated secondary antibodies (Thermo Scientific) for 1 h at room temperature. The intensities of the immunoreactive bands were detected using a SuperSignal West Femto Maximum Sensitivity Substrate Kit (Thermo Scientific). Rat anti-OPG and rabbit anti- $\beta$ -catenin monoclonal antibodies were the primary antibodies, and mouse anti- $\beta$ -actin monoclonal antibody was used as an internal reference.

### **In vitro deletion of the *$\beta$ -catenin* gene**

The in vitro deletion of the  *$\beta$ -catenin* gene was performed as described previously [24]. calvaria osteoblasts isolated from 3-day-old  *$\beta$ -catenin<sup>fx/fx</sup>* mice were seeded in 6-well culture plates at a density of  $1 \times 10^6$ /well and cultured for 6 days. Then, the cells were infected with Ad-GFP or Ad-Cre (Titer:  $4 \times 10^8$  pfu/mL; Baylor College of Medicine, Houston, TX, USA) for 72 h, and Ad-GFP was used as a control to monitor infection efficiency. After recovery for 48 h, cells were treated with or without osthole (100 mM) for 48 h. Real-time qPCR assay was performed to examine the expression of  *$\beta$ -catenin* and *OPG*. All reactions were performed in triplicate.

### **Statistical analysis**

All experiments were conducted independently at least three times. The data were expressed as mean  $\pm$  standard deviation (SD) and analyzed using SPSS 24.0 software and GraphPad Prism 8. The statistically significant differences were analyzed using Student's t-test of variance. We compared 3-month-old mice vs. 12-month-old mice and Osthole vs. vehicle. ImageJ software was employed to quantitate the grayscale intensities. \* $P < 0.05$  indicated statistically significant difference.

## **Results**

## Bone loss was severed in 12-month-old mice

3- and 12-month-old C57BL/6J mice were used to evaluate the bone mass. The  $\mu$ CT 3D image analysis on L4 showed the loss of trabecular bone in 12-month-old mice compared to that in 3-month-old mice (Fig. 1A). The quantitative analysis showed that bone volume/total volume (BV/TV) and bone mineral density (BMD) of aged mice were significantly decreased ( $P<0.05$ , Fig. 1B, 1C) compared to those in young mice, suggesting that aged mice display decreased bone mass.

## Osthole inhibited aging-induced bone loss

Osthole significantly increased the bone mass of aged mice (Fig. 2A). The quantitative analysis showed an apparent increase in 67% of BMD ( $P<0.05$ ) and 75% of BV/TV in aged mice ( $P<0.05$ ) after treatment with osthole (Fig. 2B, C) that significantly increased Tb.N ( $P<0.05$ , Fig. 2D) and decreased Tb.Sp ( $P<0.01$ , Fig. 2E). These data demonstrated that osthole inhibited aging-induced bone loss.

## Osthole inhibited osteoclast formation in aged mice

TRAP staining was performed on sections of L5. Osthole decreased the TRAP-positive number of multinucleated osteoclasts (Fig. S1A, B), and reduced the percentage of osteoclast surface in aged mice post-osthole treatment (Fig. S1C). These data showed that osthole inhibits osteoclast formation in aged mice. Conversely, we found that Osthole could not inhibit osteoclast formation in *OPG* gene knockout mice (Fig. S1D, E), suggesting that the effect of osthole might be effectuated via OPG signaling.

## Osthole inhibited osteoclastogenesis in a dose-dependent and OPG-dependent manner

OPG/RANKL signaling plays a major role in osteoclast formation. To determine the mechanism of osthole in suppressing osteoclast formation, we examined its effect on the expression of OPG and RANKL. Osthole (10, 50, 100  $\mu$ M) significantly enhanced the expression of *OPG* mRNA in a dose-dependent manner ( $P<0.05$ ), and compared with the vehicle group, a dose of 100  $\mu$ M exerted maximum effect with 3.8-fold increase (Fig. 3A). Next, we found that osthole significantly increased the protein level of OPG in a dose-dependent manner (Fig. 3B). To further determine if osthole-inhibited-osteoclastogenesis is OPG dependent, BMSCs were isolated from 3-month-old *OPG*<sup>-/-</sup> mice and the littermates of *OPG*<sup>+/+</sup> mice, cultured with M-CSF (44 ng/mL) and RANKL (100 ng/mL), plus osthole (100  $\mu$ M) or vehicle for 7 days; subsequently, TRAP staining was carried out, and the number of osteoclasts was counted. As shown in Fig. 3C and 3D, osthole significantly inhibited osteoclast formation in *OPG*<sup>+/+</sup> mice ( $P<0.05$ ). Conversely, in *OPG*<sup>-/-</sup> mice, the formation of osteoclasts was not affected. These data suggested that osthole inhibits osteoclastogenesis in an OPG-dependent manner.

## Osthole promoted the expression of OPG through activation of $\beta$ -catenin signaling

Our recent studies have demonstrated that OPG expression could be activated by  $\beta$ -catenin signaling, and osthole could activate  $\beta$ -catenin signaling [24,26,27]. First, we examined the expression of OPG and  $\beta$ -catenin expression in vivo. The immunostaining data showed that osthole significantly increased the

level of OPG (Fig. 4A, 4B) and  $\beta$ -catenin proteins (Fig. 4C, 4D) using sections of L5 samples from aged mice. To further confirm if osthole-induced-OPG expression is mediated via  $\beta$ -catenin signaling, we performed an in vitro study. Primary BMSCs were isolated from 3-month-old  $\beta$ -catenin<sup>fx/fx</sup> mice, infected with Ad-Cre or Ad-GFP, and treated with or without 100  $\mu$ M osthole. After 2 days, the total mRNA was collected, and the expression of *OPG* was detected using real-time PCR assay. We found that the deletion of  $\beta$ -catenin by Ad-Cre infection significantly inhibited osthole-induced expression of OPG (Fig. 4E), while the deletion of OPG did not affect the osthole-induced expression of the  $\beta$ -catenin protein (Fig. 4F). Taken together, these results indicated that osthole promotes the expression of OPG via  $\beta$ -catenin signaling.

## Discussion

The present study discovered that osthole inhibited bone resorption in aged mice and attenuated osteoclast formation via activated  $\beta$ -catenin-OPG signaling (Fig. 5). Osteoporosis is caused by the disorder of homeostasis between bone formation and bone resorption. Our previous results showed that osthole has the efficacy to promote osteoblastic proliferation and differentiation and act on bone metabolism [24]. Herein, we investigated whether osthole has an impact on the function of osteoclasts. It was firstly used to intervene with the elderly wild-type mice. The  $\mu$ CT analysis showed that the treatment with osthole for 4 weeks significantly increased the bone mass in senile mice. One of the major reasons for the occurrence of osteoporosis is the increased activity and quantity of osteoclasts. Thus, TRAP staining was performed, and the results demonstrated that the number of osteoclasts was decreased in senile mice after intraperitoneal injection with osthole. To further confirm this effect, the dose-dependent effect of osthole on osteoclasts, derived from primary BMSCs after M-CSF and RANKL treatment, was studied. The data showed that osthole decreases the number of osteoclasts in a dose-dependent manner. Next, we performed Immunofluorescence staining on bone slices and found that osthole attenuates the activity of functional osteoclasts. Therefore, it could be deduced that osthole inhibits osteoclast formation and osteoclast-involved bone resorptive activity.

Furthermore, we investigated the mechanism of osthole on osteoclast formation. Under normal physiological conditions, the resorption of cartilage and bone is essential for the development and regeneration of the skeleton [28]. Osteoclastogenesis is a complicated process regulated by finely orchestrated interactions between osteoclast precursors and osteoblasts/stromal cells in the bone marrow environment [29,30]. Osteoblasts produce OPG, a decoy receptor for the [receptor activator of RANKL](#). The binding of RANKL and OPG inhibits the interaction between RANKL and the receptor activator of nuclear factor-kappa B (RANK), a receptor of RANKL; therefore, OPG/RANKL/RANK plays key roles in the process of osteoclastogenesis [31,32]. The current data showed that osthole significantly promoted the expression of OPG in BMSCs in a dose-dependent manner but did not show an obvious effect on RANKL expression. RANKL is essential for osteoclast formation that is further supported by osteoblasts or their precursors [33]. Recent evidence revealed that osteocytes express high levels of RANKL and contribute to the coupling of bone formation and bone resorption [34,35]. Herein, we showed

that the osthole effects on RANKL could be indirect via overexpression of OPG, which binds with RANKL and inhibits osteoclastogenesis.

In order to demonstrate if osthole-inhibited osteoclastogenesis was OPG-dependent, we performed a rescue experiment using BMSCs from OPG<sup>+/+</sup> and OPG<sup>-/-</sup> mice. Osthole decreased the formation of osteoclasts in OPG<sup>+/+</sup> mice, while it did not affect OPG<sup>-/-</sup> mice. Therefore, the current results indicated that osthole-attenuated osteoclastogenesis was effectuated via increased expression of OPG in BMSCs. This phenomenon inhibited the binding of RANKL and RANK, but did not act on RANKL and RANK directly. The mechanism underlying osthole was further studied with respect to OPG upstream signaling. Reportedly, canonical Wnt pathway upregulates the expression of OPG in osteoblasts and chondrocytes [36,37].  $\beta$ -catenin, a key protein of the canonical Wnt pathway, is required to induce the expression of OPG in osteoblasts [38]. However, the inactivation of  $\beta$ -catenin signaling in osteoblasts increased osteoclastogenesis due to insufficient production of OPG [39]. Wnt3a cannot induce the production of normal OPG to inhibit bone resorption while lacking  $\beta$ -catenin in osteoclastic lineage [36,39]. Cellular and molecular studies have shown that  $\beta$ -catenin binding with TCF proteins regulates the expression of OPG in osteoblasts [40]. In this study, we found that osthole significantly increases the expression of  $\beta$ -catenin and OPG in BMSCs. To further discuss the interaction between  $\beta$ -catenin and OPG, we performed the in vitro rescue experiment using floxed mice( $\beta$ -catenin), and found that the deletion of the  *$\beta$ -catenin* gene inhibits osthole-induced OPG expression. These results demonstrated that osthole stimulated the expression of OPG through  $\beta$ -catenin signaling.

Canonical Wnt signaling is critical for the differentiation of mesenchymal progenitors into osteoblasts and to assess the connection between osteoblasts and bone metabolism [41]. Released  $\beta$ -catenin might also interact with site 2(-539 to -534 (TACAAAG)) and site 4(-358 to -353 (CTTTGGG)) on the OPG promoter directly, to increase the production and secretion of OPG and inhibit the binding of RANKL and RANK, thereby reducing the formation and activity of osteoclasts [40]. Reportedly, BMP2 also increases the expression of OPG by upregulating Wnt3a expression and promoting the interaction between Samd1/4 and sites 2 and 4 on OPG promoter [42]. On the other hand, Wnt5a activates the noncanonical Wnt signaling, which increases the activity of RANKL to promote osteoclastogenesis [43]. Our previous study showed that osthole significantly stimulates the expression of Wnt3a but not Wnt5a [24].

## Conclusion

Based on the findings, we concluded that osthole inhibits osteoclast formation and bone resorption by stimulating the activation of Wnt3a/ $\beta$ -catenin-OPG signaling (Fig. 5).

## Abbreviations

BMD: bone mineral density; Mx1: myxovirus resistance-1; OPG: osteoprotegerin;  $\mu$ CT: micro-computed tomography; BMSCs: bone marrow stem cells; LepR: leptin receptor; KO: knockout; WT: wild-type; DMSO:

dimethyl sulfoxide; BGP: bone gla-protein; qPCR: quantitative polymerase chain reaction; RANK: receptor activator of nuclear factor-kappa B; RANKL: the receptor activator of nuclear factor-kappa B ligand

## Declarations

### Acknowledgments

We thank the team for their cooperation.

### Authors' contributions

Conceived and designed the experiments: De-Zhi Tang

Performed the experiments: Zhen-Xiong Jin and Xin-Yuan Liao

Analyzed the data: Zhen-Xiong Jin, Xin-Yuan Liao, and Wei-Wei Da

Contributed funds/reagents/materials/analysis tools: Yong-Jian Zhao and Xiao-Feng Li

All the authors read and approved the final manuscript.

### Funding

This study was sponsored by the National Natural Science Foundation(NSFC) Gran 81973883 to De-zhi Tang and Shanghai Natural Science Foundation (19ZR1458000).

### Availability of data and materials

The datasets used and/or analyzed during the current study are available from the corresponding author on reasonable request.

### Ethics approval and consent to participate

This study has been approved by the Ethics Committee of Longhua Hospital Affiliated to Shanghai University of Traditional Chinese Medicine.

### Compliance with ethical standards

**Conflicts of interest** The authors declare that they have no conflict of interests.

### Consent for publication

Not applicable.

## References

1. Black DM, Geiger EJ, Eastell R, Vittinghoff E, Li BH, Ryan DS et al. Atypical Femur Fracture Risk versus Fragility Fracture Prevention with Bisphosphonates. *N Engl J Med*. 2020;383(8):743-53.
2. Estell EG, Rosen CJ. Emerging insights into the comparative effectiveness of anabolic therapies for osteoporosis. *Nat Rev Endocrinol*. 2020; doi: 10.1038/s41574-020-00426-5.
3. Compston JE, McClung MR, Leslie WD. Osteoporosis. *Lancet* 2019, 393(10169): 364-376.
4. Oden A, McCloskey EV, Johansson H, Kanis JA. Assessing the impact of osteoporosis on the burden of hip fractures. *Calcif Tissue Int* 2013, 92(1): 42-49.
5. Unim B, Minelli G, Da CR, Manno V, Trotta F, Palmieri L et al. Trends in hip and distal femoral fracture rates in Italy from 2007 to 2017. *Bone* 2020: 115752.
6. Leslie WD, Metge CJ, Azimae M, Lix LM, Finlayson GS, Morin SN et al. Direct costs of fractures in Canada and trends 1996-2006: a population-based cost-of-illness analysis. *J Bone Miner Res* 2011, 26(10): 2419-2429.
7. Laine JC, Novotny SA, Weber EW, Georgiadis AG, Dahl MT. Distal Tibial Guided Growth for Anterolateral Bowing of the Tibia: Fracture May Be Prevented. *J Bone Joint Surg Am* 2020; doi: 10.2106/JBJS.20.00657.
8. Khosla S, Hofbauer LC. Osteoporosis treatment: recent developments and ongoing challenges. *Lancet Diabetes Endocrinol* 2017, 5(11): 898-907.
9. Morgan EF, Unnikrisnan GU, Hussein AI. Bone Mechanical Properties in Healthy and Diseased States. *Annu Rev Biomed Eng* 2018, 20: 119-143.
10. Li B, Liu M, Wang Y, Gong S, Yao W, Li W et al. Puerarin improves the bone micro-environment to inhibit OVX-induced osteoporosis via modulating SCFAs released by the gut microbiota and repairing intestinal mucosal integrity. *Biomed Pharmacother* 2020; 132:110923.
11. Compston JE. Sex steroids and bone. *Physiol Rev* 2001, 81(1): 419-447.
12. Yun C, Wu S, Xin-xin Z, Yan-die L, Hao C, Hao LI. Osthole prevents acetaminophen-induced liver injury in mice. *Acta Pharmacol Sin* 2018, 39(1): 74-84.
13. Zhang Z, Leung W, Li G, Kong S, Lu X, Wong Y et al. Osthole Enhances Osteogenesis in Osteoblasts by Elevating Transcription Factor Osterix via cAMP/CREB Signaling In Vitro and In Vivo. *Nutrients* 2017, 9(6): 588.
14. Dai X, Yin C, Zhang Y, Guo G, Zhao C, Wang O et al. Osthole inhibits triple negative breast cancer cells by suppressing STAT3. *J Exp Clin Cancer Res* 2018, 37(1):322.
15. Hassanein E, Sayed AM, Hussein OE, Mahmoud AM. Coumarins as Modulators of the Keap1/Nrf2/ARE Signaling Pathway. *Oxid Med Cell Longev* 2020:1675957.
16. Gao LN, An Y, Lei M, Li B, Yang H, Lu H et al. The effect of the coumarin-like derivative osthole on the osteogenic properties of human periodontal ligament and jaw bone marrow mesenchymal stem cell sheets. *Biomaterials* 2013, 34(38): 9937-9951.
17. Ma Y, Ran D, Cao Y, Zhao H, Song R, Zou H et al. The effect of P2X7 on cadmium-induced osteoporosis in mice. *J Hazard Mater* 2020: 124251.

18. Kfoury Y, Scadden DT. Mesenchymal cell contributions to the stem cell niche. *Cell Stem Cell* 2015, 16(3): 239-253.
19. Xu R, Yallowitz A, Qin A, Wu Z, Shin DY, Kim JM et al. Targeting skeletal endothelium to ameliorate bone loss. *Nat Med* 2018, 24(6): 823-833.
20. Curtis M, Kenny HA, Ashcroft B, Mukherjee A, Johnson A, Zhang Y et al. Fibroblasts Mobilize Tumor Cell Glycogen to Promote Proliferation and Metastasis. *Cell Metab* 2019, 29(1): 141-155.
21. Park D, Spencer JA, Koh BI, Kobayashi T, Fujisaki J, Clemens TL et al. Endogenous bone marrow MSCs are dynamic, fate-restricted participants in bone maintenance and regeneration. *Cell Stem Cell* 2012, 10(3): 259-272.
22. Zhou BO, Yue R, Murphy MM, Peyer JG, Morrison SJ. Leptin-receptor-expressing mesenchymal stromal cells represent the main source of bone formed by adult bone marrow. *Cell Stem Cell* 2014, 15(2): 154-168.
23. Worthley DL, Churchill M, Compton JT, Tailor Y, Rao M, Si Y et al. Gremlin 1 identifies a skeletal stem cell with bone, cartilage, and reticular stromal potential. *Cell* 2015, 160(1-2): 269-284.
24. Tang DZ, Hou W, Zhou Q, Zhang M, Holz J, Sheu TJ et al. Osteole stimulates osteoblast differentiation and bone formation by activation of beta-catenin-BMP signaling. *J Bone Miner Res* 2010, 25(6): 1234-1245.
25. Jin Z, Chen J, Shu B, Xiao Y, Tang D. Bone mesenchymal stem cell therapy for ovariectomized osteoporotic rats: a systematic review and meta-analysis. *BMC Musculoskelet Disord* 2019, 20(1): 556.
26. Yan Y, Tang D, Chen M, Huang J, Xie R, Jonason JH et al. Axin2 controls bone remodeling through the beta-catenin-BMP signaling pathway in adult mice. *J Cell Sci* 2009, 122(Pt 19): 3566-3578.
27. Zhu M, Tang D, Wu Q, Hao S, Chen M, Xie C et al. Activation of beta-catenin signaling in articular chondrocytes leads to osteoarthritis-like phenotype in adult beta-catenin conditional activation mice. *J Bone Miner Res* 2009, 24(1): 12-21.
28. Tsukasaki M, Takayanagi H. Osteoimmunology: evolving concepts in bone-immune interactions in health and disease. *Nat Rev Immunol* 2019, 19(10): 626-642.
29. Shin CS, Her SJ, Kim JA, Kim DH, Kim SW, Kim SY et al. Dominant negative N-cadherin inhibits osteoclast differentiation by interfering with beta-catenin regulation of RANKL, independent of cell-cell adhesion. *J Bone Miner Res* 2005, 20(12): 2200-2212.
30. Charles JF, Aliprantis AO. Osteoclasts: more than 'bone eaters'. *Trends Mol Med* 2014, 20(8): 449-459.
31. Lacey DL, Boyle WJ, Simonet WS, Kostenuik PJ, Dougall WC, Sullivan JK et al. Bench to bedside: elucidation of the OPG-RANK-RANKL pathway and the development of denosumab. *Nat Rev Drug Discov* 2012, 11(5): 401-419.
32. Feng X, McDonald JM. Disorders of bone remodeling. *Annu Rev Pathol* 2011, 6: 121-145.

33. Lv WT, Du DH, Gao RJ, Yu CW, Jia Y, Jia ZF et al. Regulation of Hedgehog signaling Offers A Novel Perspective for Bone Homeostasis Disorder Treatment. *Int J Mol Sci* 2019, 20(16):3981.
34. Davaine JM, Quillard T, Chatelais M, Guilbaud F, Brion R, Guyomarch B et al. Bone Like Arterial Calcification in Femoral Atherosclerotic Lesions: Prevalence and Role of Osteoprotegerin and Pericytes. *Eur J Vasc Endovasc Surg* 2016, 51(2): 259-267.
35. Kadriu B, Gold PW, Luckenbaugh DA, Lener MS, Ballard ED, Niciu MJ et al. Acute ketamine administration corrects abnormal inflammatory bone markers in major depressive disorder. *Mol Psychiatry* 2018, 23(7): 1626-1631.
36. Wang B, Jin H, Zhu M, Li J, Zhao L, Zhang Y et al. Chondrocyte beta-catenin signaling regulates postnatal bone remodeling through modulation of osteoclast formation in a murine model. *Arthritis Rheumatol* 2014, 66(1): 107-120.
37. Appelman-Dijkstra NM, Papapoulos SE. Clinical advantages and disadvantages of anabolic bone therapies targeting the WNT pathway. *Nat Rev Endocrinol* 2018, 14(10): 605-623.
38. Sato A, Shimizu M, Goto T, Masuno H, Kagechika H, Tanaka N et al. WNK regulates Wnt signalling and beta-Catenin levels by interfering with the interaction between beta-Catenin and GID. *Commun Biol* 2020, 3(1):
39. Albers J, Keller J, Baranowsky A, Beil FT, Catala-Lehnen P, Schulze J et al. Canonical Wnt signaling inhibits osteoclastogenesis independent of osteoprotegerin. *J Cell Biol* 2013, 200(4): 537-549.
40. Glass DN, Bialek P, Ahn JD, Starbuck M, Patel MS, Clevers H et al. Canonical Wnt signaling in differentiated osteoblasts controls osteoclast differentiation. *Dev Cell* 2005, 8(5): 751-764.
41. Fan J, Lee CS, Kim S, Zhang X, Pi-Anfruns J, Guo M et al. Trb3 controls mesenchymal stem cell lineage fate and enhances bone regeneration by scaffold-mediated local gene delivery. *Biomaterials* 2021, 264:
42. Sato MM, Nakashima A, Nashimoto M, Yawaka Y, Tamura M. Bone morphogenetic protein-2 enhances Wnt/beta-catenin signaling-induced osteoprotegerin expression. *Genes Cells*. 2009;14(2):141-53.
43. Maeda K, Kobayashi Y, Udagawa N, Uehara S, Ishihara A, Mizoguchi T et al. Wnt5a-Ror2 signaling between osteoblast-lineage cells and osteoclast precursors enhances osteoclastogenesis. *Nat Med*. 2012;18(3):405-12.

## Figures

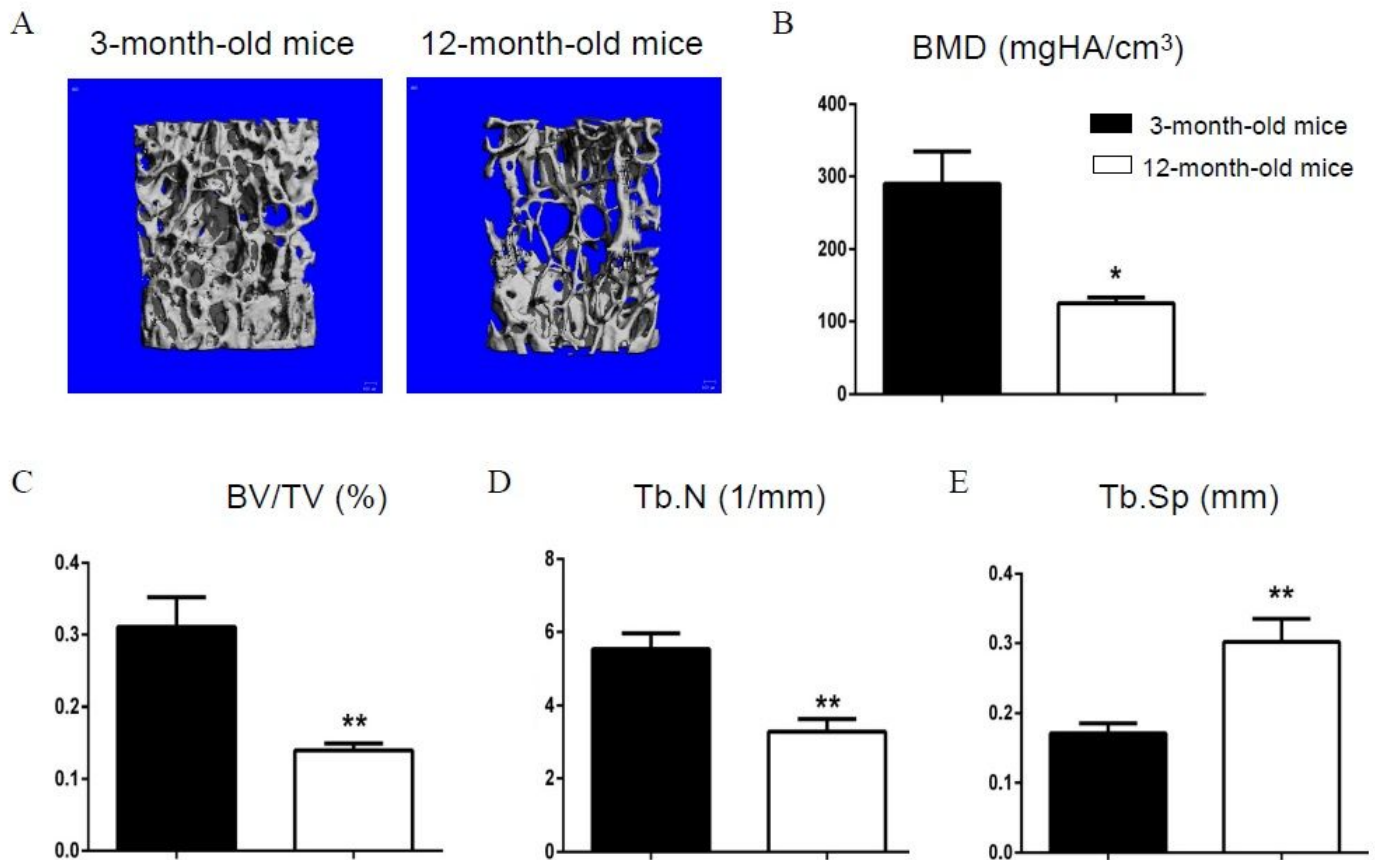


**Figure 1**

Bone mass was significantly reduced in 12-month-old mice. Three-month-old and 12-month-old C57BL/6 mice were used to evaluate the bone mass. (A) The  $\mu$ CT 3D image analysis of the fourth lumbar vertebra (L4) demonstrated an apparent bone loss in 12-month-old mice compared to 3-month-old mice. The quantitative analysis showed that bone volume (BV) and bone mineral density (BMD) were significantly decreased in 12-month-old mice compared to 3-month-old mice (B and C, n=6). \*P<0.05, \*\*P<0.01, unpaired Student's t-test (3-month-old mice vs. 12-month-old mice).

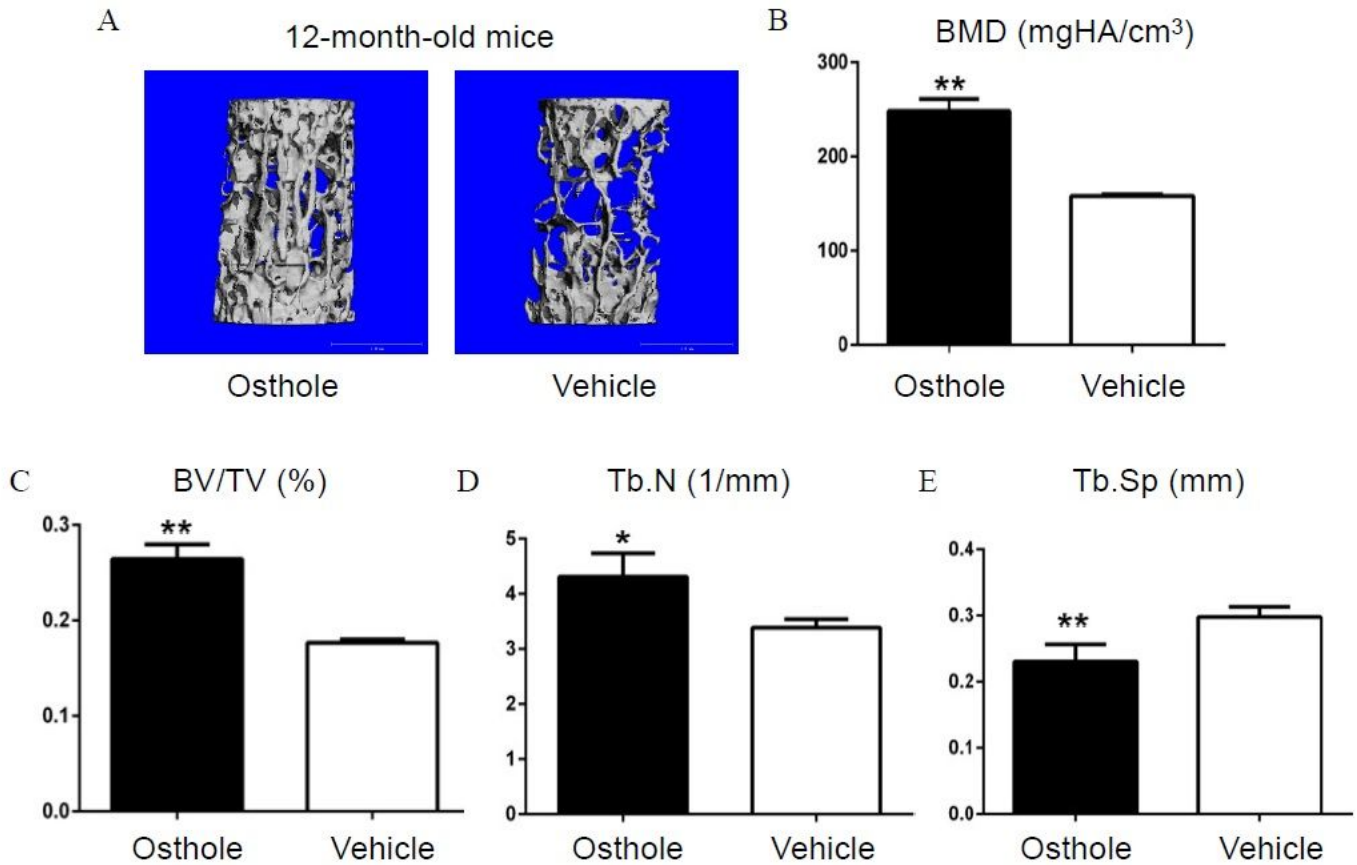


**Figure 2**

Osthole significantly increased the bone mass of aged mice. Twelve-month-old C57BL/6J mice were treated with Osthole (5 mg/kg/day) or vehicle (corn oil) by intraperitoneal injection once a day for 4 weeks. Then, mice were sacrificed, and the lumbar vertebrae were harvested for evaluation. (A) The  $\mu$ CT 3D image analysis of L4 samples showed that osthole significantly increased bone mass in aged mice. (B and C) An apparent increase in bone volume (BV) and bone mineral density (BMD) was observed in aged mice after treatment with osthole by the quantitative analysis (n=6). (D and E) Osthole was found to significantly increase Tb.N ( $P<0.05$ ) and decreased Tb.Sp ( $P<0.05$ ). \* $P<0.05$ , \*\* $P<0.01$ , unpaired Student's t-test (osthole vs. vehicle).

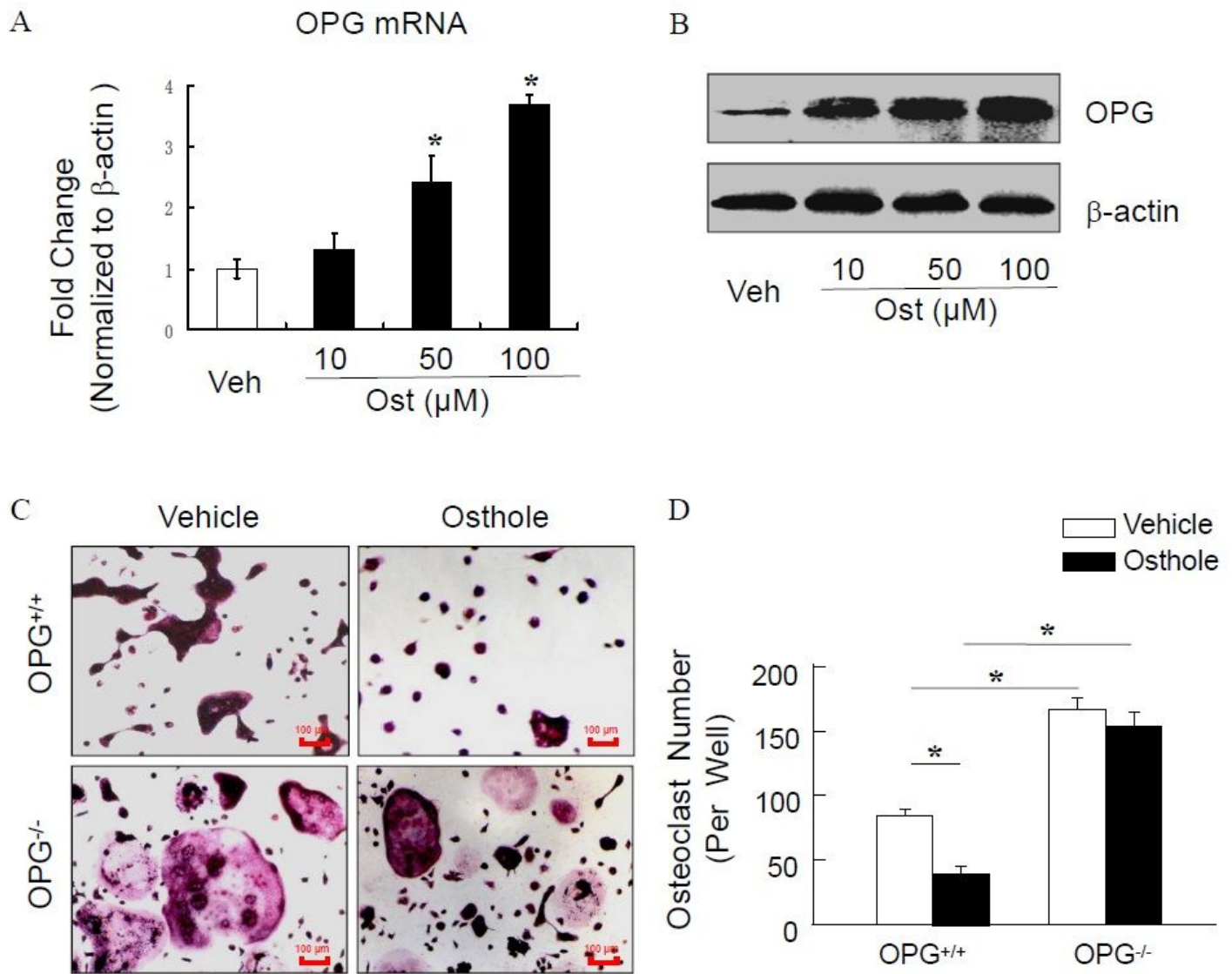


**Figure 3**

Osthole inhibits osteoclastogenesis in a dose-dependent and OPG-dependent manner. (A) Osteoblasts were cultured and treated with various doses of Osthole (10–100 μM) or vehicle (DMSO) for 2 days; OPG expression was detected using real-time PCR assay. All assays were performed in triplicate and repeated three times. Data were expressed as mean±S.D. \*P<0.05, unpaired Student’s t-test (osthole vs. vehicle). (B) The protein expression of OPG was detected using Western blot assay. A and B showed that osthole significantly increased the mRNA and protein level of OPG in a dose-dependent manner, with the maximum effect at the dose of 100 μM. (C) BMSCs were isolated from 3-month-old OPG<sup>-/-</sup> mice and the littermates of OPG<sup>+/+</sup> mice, cultured with M-CSF (44 ng/mL) and RANKL (100 ng/mL), plus Osthole (100 μM) or vehicle for 7 days, and then, TRAP staining was performed. All assays were performed in triplicate and repeated three times. One representative view from each condition is shown. The scar bar is 100μm. (D) Quantification of osteoclast number for osthole in (C). The number of multinucleated TRAP-positive cells (>3 nuclei) in each representative view area at ×40 magnification. Bars show an average of three

replicates, and data were expressed as mean±S.D. \*P<0.05, unpaired Student's t-test. (C and D) showed that osthole inhibited the formation of osteoclasts in an OPG-dependent manner.

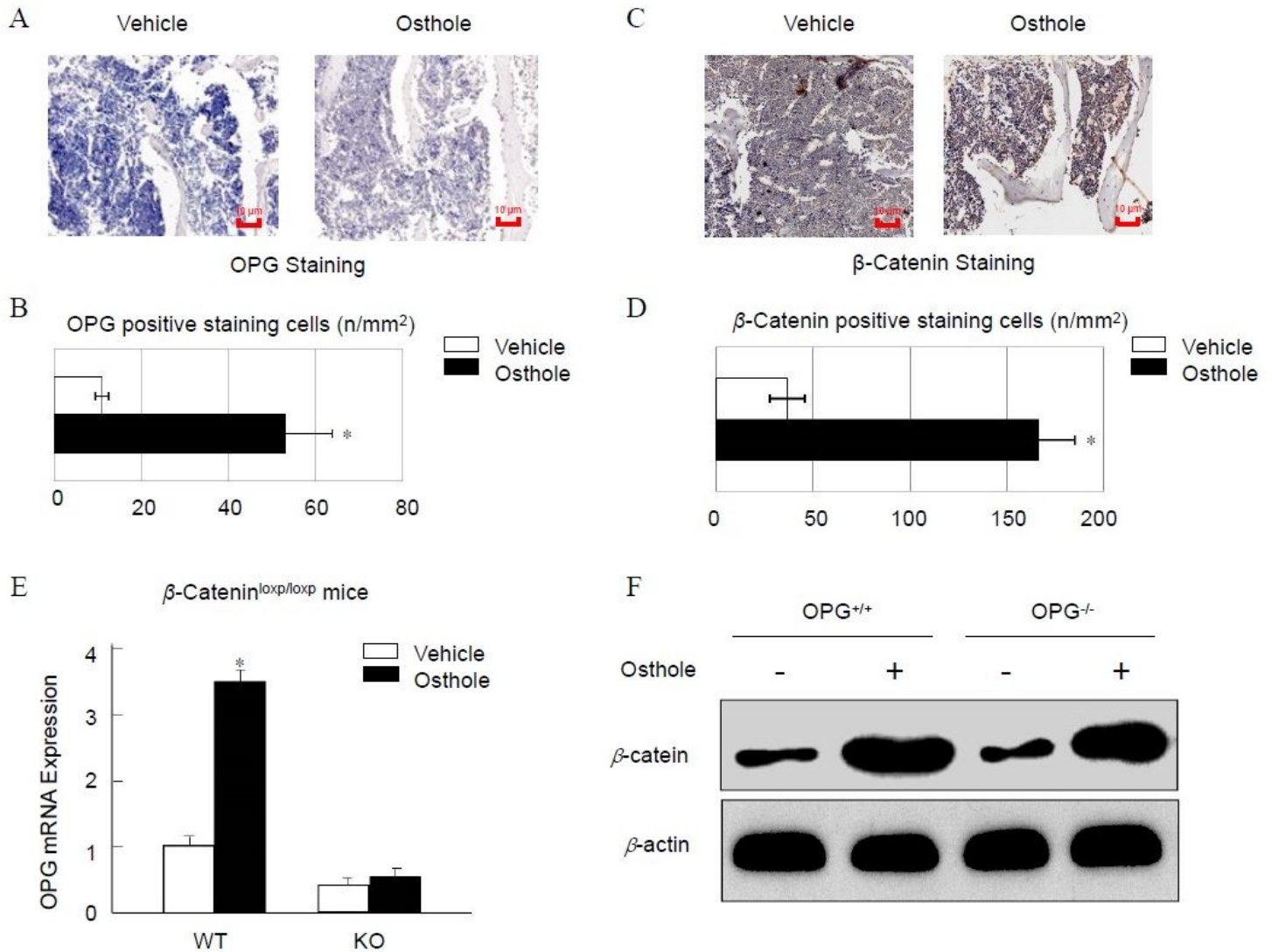


**Figure 4**

Osthole promotes the expression of OPG through activation of  $\beta$ -catenin signaling. (A) Twelve-month-old C57BL/6 mice were treated with osthole (5 mg/kg/day) or vehicle (corn oil) by intraperitoneal injection once a day. Mice were sacrificed after 4 weeks, sections of the L5 were prepared. The scar bar is 10 $\mu$ m. (B) OPG immunostaining was performed. Osthole increased the OPG protein level in aged mice. (C)  $\beta$ -catenin immunostaining was performed in L5 sections of 12-month-old C57BL/6 mice. The scar bar is 10 $\mu$ m. (D) Osthole increased the  $\beta$ -catenin protein level in aged mice. (E) Osteoblasts were isolated from 3-day-old  $\beta$ -catenin<sup>loxP/loxP</sup> mice, infected with Ad-Cre or Ad-GFP, and treated with or without 100  $\mu$ M osthole. After 2 days, the total mRNA was collected and the expression of OPG was detected using real-time PCR assay. All assays were performed in triplicate and repeated three times. Data were expressed as mean±SD. \*P<0.05, unpaired Student's t-test (osthole vs. vehicle). The deletion of  $\beta$ -catenin by Ad-Cre infection significantly inhibited osthole-induced expression of OPG. (F) Osteoblasts were isolated from 3-day-old OPG<sup>-/-</sup> mice and the littermates of OPG<sup>+/+</sup> mice were treated with osthole (100  $\mu$ M) or vehicle for

2 days; the total protein was collected and the expression of  $\beta$ -catenin was detected using the Western blot assay. The deletion of OPG did not affect osthole-induced expression of  $\beta$ -catenin protein.

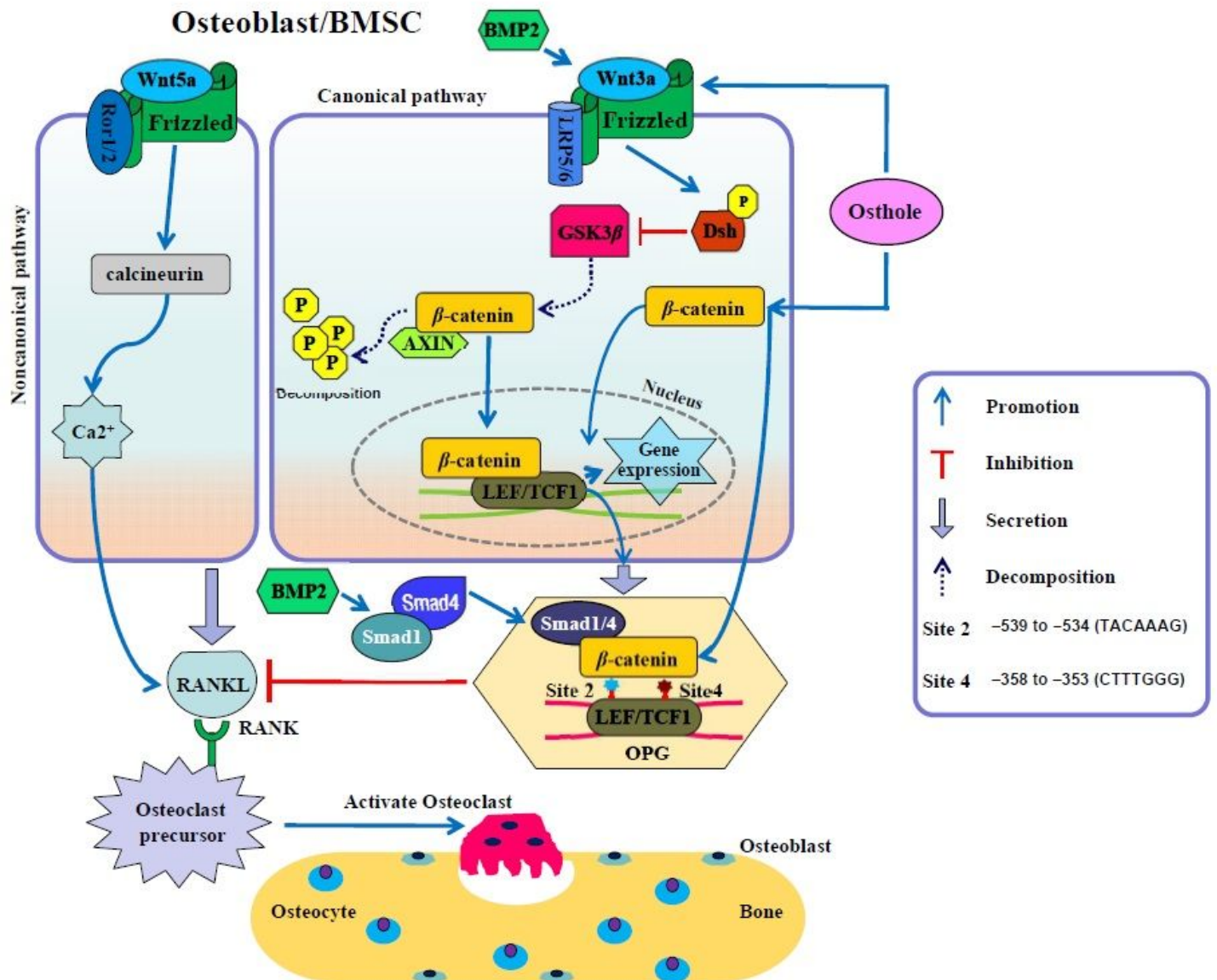


**Figure 5**

Schematic of the mechanism underlying Osthole-mediated inhibition of osteoclast formation and bone resorption.

## Supplementary Files

This is a list of supplementary files associated with this preprint. Click to download.

- [TableS1revisedversion1.pdf](#)